Macromolecules

Article

pubs.acs.org/Macromolecules

Self-Assembly Assisted Polypolymerization (SAAP) of Diblock Copolymer Chains with Two Reactive Groups at Its Insoluble End

Lianwei Li,[†,*] Manqing Yan,[†] Guangzhao Zhang,[†] and Chi Wu[†,‡,*]

[†]Hefei National Laboratory for Physical Sciences at Microscale, Department of Chemical Physics, University of Science and Technology of China, Hefei, China 230026

[‡]Department of Chemistry, The Chinese University of Hong Kong, Shatin N.T., Hong Kong

Supporting Information

ABSTRACT: Preparation of diblock copolymers, (≡,N_3)-poly(*N*-isopropylacrylamide)-*b*-poly(*N*,*N*-dimethylacrylamide) [(≡,N_3)-PNIPAM-*b*-PDMA] and (≡,N_3)-polystyrene-*b*-PNIPAM [(≡,N_3)-PS-*b*-PNIPAM], with reactive alkyne and azide at one end using a trifunctional agent enables us to study how their self-assembly in a selective solvent affects interchain coupling, i.e., the self-assembly assisted polypolymerization (SAAP). As expected, (≡,N_3)-PNIPAM-*b*-PDMA chains self-assemble into a micelle-like core−shell structure with a PNIPAM core in water at 50 °C. The coupling of as many as 17 PNIAPM ends together led to star-like chains, independent of the copolymer concentration, while the coupling efficiencies at lower temperatures (with no self-assembly) and in good solvents are much lower. These star-like chains remember their "birth" state in water and undergo the intrachain contraction to form single-chain micelles instead of large multichain aggregates. On the other hand, (≡,N_3)-PS-*b*-PNIPAM exists as individual chains in THF, a mixture of unimers and micelles in 2-propanol, the core−shell micelles in methanol, and irregular aggregates in water. Only in methanol, the coupling efficiency is notably improved. The addition of water into 2-propanol enhances the self-assembly and so does the interchain coupling. The current study shows that even the solvophobic interaction makes the insoluble blocks less mobile inside the core and decreases the collision probability of reactive chain ends, the self-assembly still concentrates the reactive ends together and assists the coupling if the selective solvent is properly chosen.

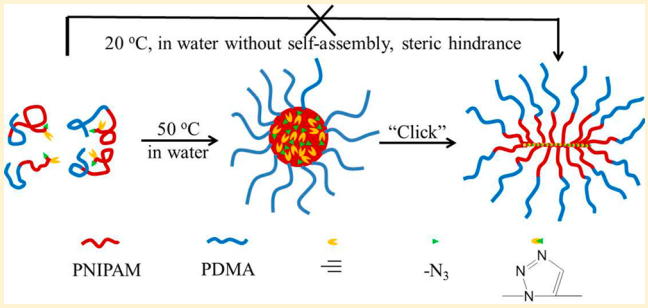

INTRODUCTION

In polymer science, coupling reactions based on step-growth mechanism have been widely used to construct polymers with different topologies in the past two decades, e.g., cyclic,[1,2] star,[3] graft,[4] and multiblock (co)polymers.[5] Meanwhile, various types of coupling reactions were adopted, such as the esterification,[6−8] Williamson reaction,[9−11] Suzuki coupling reaction,[12,13] and "click" chemistry[14−16] to name but a few. However, even considering the versatile nature of the "click" reaction, the overall interchain coupling efficiency of long macromonomers in good solvents is generally low due to steric hindrance, especially when their weight-average molar masses (M_w) are higher than ~10^4 g/mol. Namely, for most of the chains, their reactive ends are wrapped and hidden inside a coiled conformation. Such a low coupling efficiency is a drawback of the widely adopted "arm-first"[17−20] and "graft-onto"[21−24] strategies for constructing comb-like and star-like (co)polymers in dilute solutions.

Essentially, the key to the high interchain coupling efficiency is to concentrate the reactive ends in a small volume and expose them to each other. It has been well-known in polymer physics that the self-assembly of block copolymer chains in a selective solvent can form core−shell micelles.[25−27] Such a self-assembly forces the reactive chain ends of soluble or insoluble blocks to stay on the periphery or in the core of each micelle. In principle, it should make the interchain coupling much easier. Previously, we have successfully prepared multiblock $(A-B-A)_n$ copolymers by the self-assembly assisted polypolymerization (SAAP) of A−B−A triblock precursors with one reactive group at one end of A-block in a solvent selectively poor for the middle B-block so that the two reactive groups are concentrated and forced to stick out on the periphery.[28−31] Similarly, the multiblock $(PEO-PPO-PEO)_5$ was prepared by concentrating the azide and alkyne groups of equimolar N_3−PEO-*b*-PPO-*b*-PEO-N_3 and HC≡C-PEO-*b*-PPO-*b*-PEO-C≡CH chains on the periphery in water, a solvent selectively poor for the PPO block at higher temperature.[30] We also prepared the multiblock $(PI-PS-PI)_{30}$ using esterification between diamine and diacyl chloride groups in *n*-hexane, a solvent selectively poor for PS.[31] It is worth noting that similar self-assembly assisted reaction strategy was used to construct nanoparticles,[32,33] star polymers,[32] tadpole polymers,[34,35] and macrocyclic polymers;[36] but they were based on the chain-

Received: August 9, 2013
Revised: September 17, 2013
Published: September 30, 2013

   dx.doi.org/10.1021/ma401675q | *Macromolecules* 2013, 46, 8152−8160

growth mechanism, which resulted in corsslinked structures, totally different with what we discussed in the current work.

In comparison with the interchain coupling on the periphery, the reaction inside the core is more complicated but one does not have a choice because of the solvent selection. Inside the core, the insoluble blocks move much slower, reducing the collision probability of the reactive groups; on the other hand, the self-assembly concentrates the reactive ends inside a small volume (<10 nm^3), promoting the interchain coupling. It is clear that in a completely "frozen" core, the former should play a dominant role so that the interchain coupling would practically cease, but increasing the solubility of the blocks inside the core leads to a smaller aggregation number, i.e., a lower concentration of the reactive ends, and reduces the interchain coupling efficiency. Therefore, there must exist a delicae balance between these two opposite effects. The current experiments were designed to find how the selective solvent (solubility) affects the interchain coupling efficiency in the SAAP.

Note that the interchain coupling of the insoluble blocks inside the core results in a star-like copolymer chain instead of linear multiblock chains previously reported,[30,31] as schemetically shown in Scheme 1. There are different ways to design and prepare the reactive groups at the end of the insoluble block. In the current study, we prepared a novel trifunctional agent with three groups: alkyne, bromine and thiocarbonylthio and used it to prepare copolymers (≡,Br)-poly(*N*-isopropylacrylamide)-*b*-poly(*N*,*N*-dimethylacrylamide) [(≡,Br)-PNIPAM-*b*-PDMA] by using successive reversible addition−fragmentation chain transfer polymerization (RAFT) (Scheme 2). After using radical-addition−fragmentation coupling (RAFC) to remove the thiocarbonylthio group and replacing the remaining bromine by azide moieties, we obtained linear (≡,N_3)-PNIPAM-*b*-PDMA copolymer with the end of its PNIPAM block simultaneously attached with two reactive groups; one is alkyne and the other is azide.

In a solvent selectively poor for PNIPAM, e.g., water at temperatures higher than 32 °C, such a diblock copolymer can self-assemble into a core−shell micelle-like structure with a collapsed PNIPAM core and a swollen PDMA shell. The effect of the self-assembly on the interchain coupling of (≡,N_3)-PNIPAM-*b*-PDMA inside the core in aqueous solutions was studied by different methods, including the Fourier transform infrared spectroscopy (FT-IR), size exclusion chromatography (SEC), and laser light scattering (LLS). Further, we studied the association of the star-like chains prepared by the SAAP in solutions. Similarly, (≡,N_3)-polystyrene-*b*-poly(*N*-isopropylacrylamide) [(≡,N_3)-PS-*b*-PNIPAM] was prepared and studied in different solvents and solvent mixtures.

Scheme 1. Schematic of Interchain Coupling of (≡,N_3)-PNIPAM-*b*-PDMA with and without Self-Assembly Assisted Polypolymerization (20 and 50 °C)

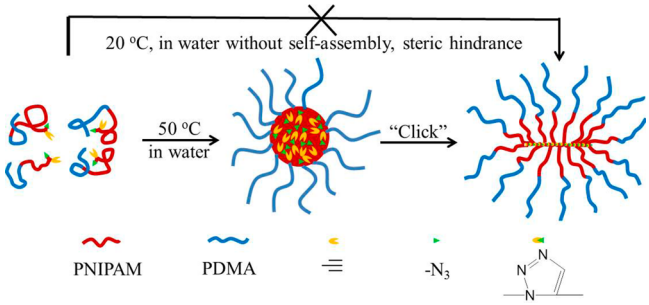

EXPERIMENTAL SECTION

Materials. *N*-Isopropylacrylamide (NIPAM) was recrystallized twice in a mixture of hexane and toluene (40/60, v/v%). *N*,*N*-dimethylacrylamide (DMA), styrene (St), dioxane, THF, methanol and 2-propanol were vacuum distilled from calcium hydride (CaH_2). Dimethylformamide (DMF) was distilled from anhydrous $MgSO_4$. 2,2-azobis(isobutyronitrile) (AIBN) was recrystallized twice in ethanol. Benzoyl peroxide (BPO) was recrystallized twice in a mixture of methanol and chloroform. Other chemicals and reagents were used as received without further purification unless otherwise stated.

Characterization. ^1H nuclear magnetic resonance (NMR) spectra were recorded on a Bruker AV400 spectrometer by using deuterated chloroform ($CDCl_3$) as solvent and tetramethylsilane (TMS) as an internal standard. The FT-IR spectra were recorded on a Bruker

Scheme 2. Schematic of Synthesis of Two Diblock Copolymers with Reactive Ends

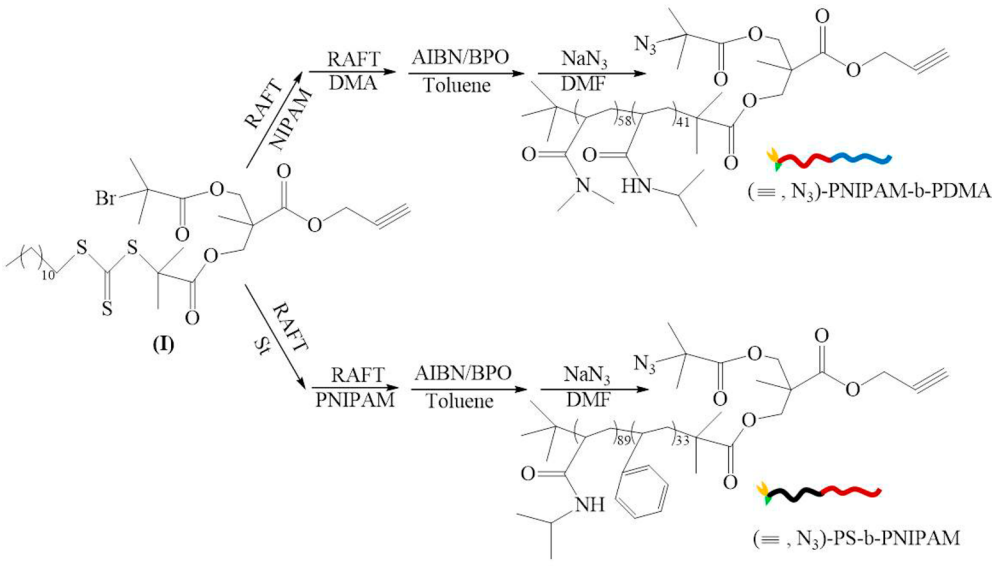

dx.doi.org/10.1021/ma401675q | *Macromolecules* 2013, 46, 8152−8160

VECTOR-22 IR spectrometer. The spectra were collected over 64 scans with a spectral resolution of 4 cm^{-1}. The number- and weight-average molar masses ($M_{n,SEC}$ and $M_{w,SEC}$) were determined at 35 °C by using SEC (Waters 1515) that is equipped with three Waters Styragel columns (HT2, HT4, and HT6), a refractive index detector (RI, Wyatt WREX-02), and a conventional calibration with polystyrene standards and DMF as eluent with a flow rate of 1.0 mL/min.

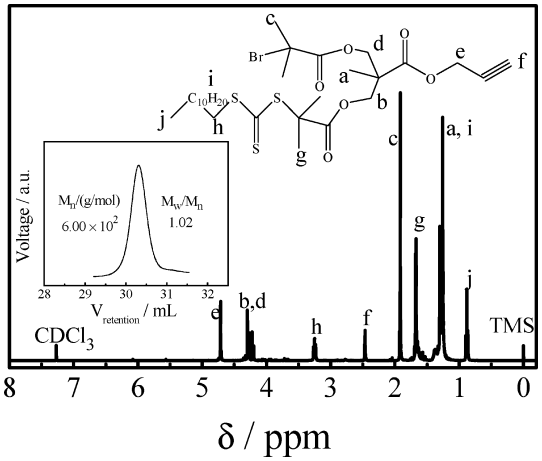

Figure 1. ^{1}H NMR spectrum and SEC curve (inset) of trifunctional RAFT agent (**I**) with one alkyne, one bromine, and one thiocarbonylthio groups.

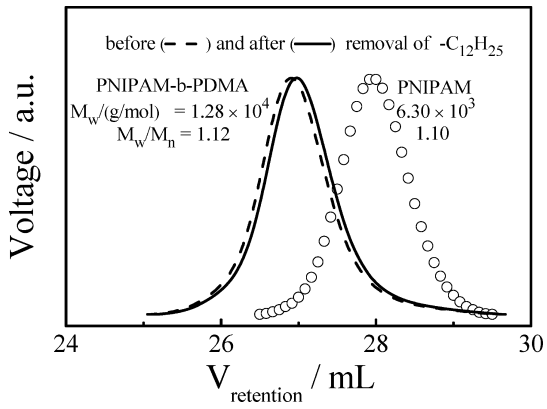

Figure 2. SEC curves of PNIPAM and PNIPAM-*b*-PDMA-$C_{12}H_{25}$ before and after treated with a mixture of AIBN and BPO.

A commercial LLS spectrometer (ALV/DLS/SLS-5022F) equipped with a multiτ digital time correlator (ALV5000) and a cylindrical 22 mW UNIPHASE He−Ne laser (λ_0 = 632.8 nm) as the light source was used. The apparent weight-average molar mass ($M_{w,LLS}$) of star-like polymers was determined by using a dilute solution (1.0 g/L in THF) at T = 25 °C, where we ignored the small polymer concentration correction. Before LLS characterization, each solution was clarified with a 200-nm PTFE filter (Millipore) to remove dusts and further centrifuged at 6000 rpm for 20 min. At 25 °C, the specific refractive index increments (dn/dc) of PNIPAM-*b*-PDMA are 0.115 mL/g in THF and 0.158 in water; of PS-*b*-PNIPAM are 0.127 in THF, 0.156 in methanol and 0.150 in a mixture of water/2-propanol; 0.190 in water (20 °C) estimated from the additive rule: $dn/dc = W_{PS}\% \times (dn/dc)_{PS} + W_{PNIPAM}\% \times (dn/dc)_{PNIPAM}$, where dn/dc_{PS} and dn/dc_{PNIPAM} in water are 0.256 mL/g and 0.168 mL/g, respectively. The absolute viscosity (η) of the mixture of water and 2-propanol (v/v) was measured by using a Ubbelohde capillary viscometer and η = 2.04 cP (0/10), 2.06 (1/9), 2.11 (2/8), and 2.39 (3/7).

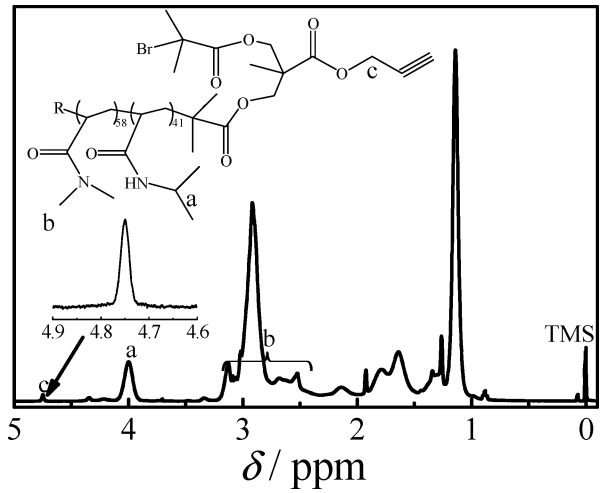

Figure 3. ^{1}H NMR spectrum of diblock copolymer (≡,Br)-PNIPAM-*b*-PDMA in $CDCl_3$.

Synthesis of First Block (≡,Br)-PNIPAM by RAFT Polymerization. A three-necked flask equipped with a magnetic stirring bar and three rubber septums was charged with RAFT agent (**I**) (0.25 g, 0.375 mmol), NIPAM (4.25 g, 37.5 mmol), AIBN (6.1 mg, 0.0375 mmol), and dioxane (20 mL). The flask was degassed by three freeze−pump−thaw cycles and then placed in an oil bath (60 °C) under nitrogen atmosphere. After 3 h, the flask was cooled and the reaction mixture was concentrated before the resultant polymer was precipitated twice in an excess amount of cold ether and dried in a vacuum oven overnight at 40 °C. The polystyrene precursor, (≡,Br)-PS, was synthesized in a similar fashion by the RAFT polymerization.

Synthesis of Copolymer (≡,Br)-PNIPAM-b-PDMA by RAFT Polymerization. A three-necked flask equipped with a magnetic stirring bar and three rubber septums was charged with (≡,Br)-PNIPAM (1.0 g, 0.18 mmol), DMA (1.83 g, 18 mmol), AIBN (2.9 mg, 0.018 mmol) and dioxane (10 mL). The flask was degassed by three freeze−pump−thaw cycles and then placed in an oil bath (60 °C) under nitrogen atmosphere. After 3 h, the flask was cooled and the reaction mixture was concentrated before the resultant diblock copolymer was precipitated twice into an excess amount of cold ether and dried in a vacuum oven overnight at 40 °C. The diblock linear copolymer, (≡,Br)-PS-*b*-PNIPAM, was synthesized in a similar fashion.

Removal of Thiocarbonylthio Group. The typical procedure is outlined as follows. A mixture of (≡,Br)-PNIPAM-*b*-PDMA (1.7 g, 0.18 mmol), AIBN (1.3 g, 50 mol equiv), BPO (0.08 g, 2 mol equiv) and toluene (10 mL) was placed in an ampule. The solution was degassed through three freeze−pump−thaw cycles, sealed, and heated at 80 °C for 4 h. The ampule was opened and the copolymer was precipitated twice into an excess amount of cold ether and then dried in a vacuum oven overnight at 40 °C. In this way, (≡,Br)-PNIPAM-*b*-PDMA without the thiocarbonylthio group was obtained. The removal of the thiocarbonylthio group from (≡,Br)-PS-*b*-PNIPAM was done similarly.

Synthesis of (≡,N_3)-PNIPAM-b-PDMA by Azidation. Into a 50-mL round-bottom flask were charged (≡,Br)-PNIPAM-*b*-PDMA (1.3 g, 0.12 mmol), DMF (10 mL), and NaN_3 (0.082 g, 1.2 mmol) under N_2. The solution mixture was stirred at room temperature for 24 h. After removing most of the solvent under a reduced pressure, the remaining solution mixture was diluted with CH_2Cl_2 and then passed through a filter paper funnel to remove residual sodium salts. The resultant (≡,N_3)-PNIPAM-*b*-PDMA was precipitated into an excess amount of cold ether and dried in a vacuum oven overnight at the room temperature. The conversion from (≡,Br)-PS-*b*-PNIPAM to (≡,N_3)-PS-*b*-PNIPAM was done by a similar azidation procedure.

Interchain Coupling of (≡,N_3)-PNIPAM-b-PDMA via SAAP. The general procedure was as follows. Into a 20-mL three-necked round-

dx.doi.org/10.1021/ma401675q | Macromolecules 2013, 46, 8152−8160

bottom flask, (≡,N_3)-PNIPAM-*b*-PDMA diblock copolymer (0.1 g, 0.0095 mmol) and H_2O (10 mL) were added. After the dissolution was complete at the room temperature, nitrogen was bubbled into the solution to remove oxygen for ~30 min, The flask was placed in an oil bath thermostated at 50 °C for ~30 min to induce the self-assembly before adding sodium ascorbate (0.025 g, 0.12 mmol) and $CuSO_4$ (10 mg, 0.06 mmol). The reaction mixture was stirred at 50 °C for 24 h under N_2. After removing all the solvents under a reduced pressure, we dissolved the residues in THF and filtered through an alumina column. The resultant star-like copolymer (PNIPAM-*b*-PDMA)$_n$ was precipitated in an excess amount of cold ether and dried in vacuum overnight at the room temperature.

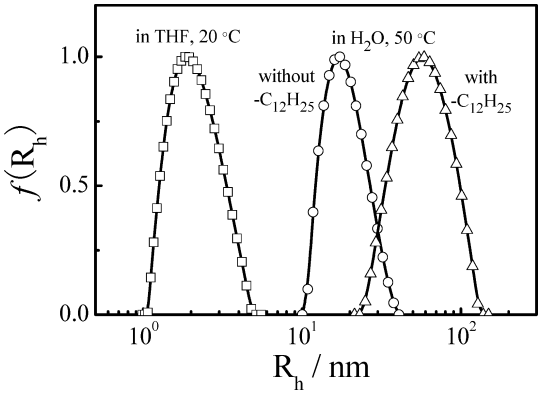

Figure 4. Hydrodynamic radius distributions ($f(R_h)$) of PNIPAM-*b*-PDMA-$C_{12}H_{25}$ in THF at 20 °C and in water at 50 °C before and after removal of $-C_{12}H_{25}$ end.

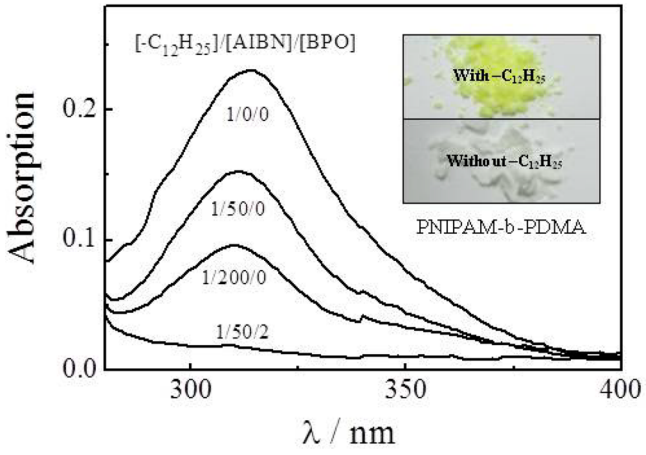

Figure 5. UV spectra of PNIPAM-*b*-PDMA-$C_{12}H_{25}$ treated with different mixtures of AIBN and BPO in THF to remove $-C_{12}H_{25}$ end.

The interchain coupling of (≡,N_3)-PS-*b*-PNIPAM via the SAAP was carried out in methanol, 2-propanol, 2-propanol/water and water, respectively. The general procedure was as follows. In a 20-mL three-necked round-bottom flask, (≡,N_3)-PS-*b*-PNIPAM (0.05 g) and oxygen-free methanol (10 mL) were added. After the solution was heated at 60 °C under a N_2 positive pressure for 2 h, the flask was cooled down to 25 °C and then PMDETA (29 μL) and CuBr (20 mg) were added. The reaction mixture was stirred under a flow N_2 for 10 min and then a positive N_2 pressure for 24 h. After the removal of all the solvents under a reduced pressure, the residues were dissolved in THF and filtered by an alumina column. The resultant copolymer (PS-*b*-PNIPAM)$_n$ was precipitated in an excess amount of cold ether and dried in vacuum overnight at the room temperature.

In water, (≡,N_3)-PS-*b*-PNIPAM (0.005 g) was first dissolved in 2 mL of THF and then dropped into 50 mL of water at ~10 °C by a programmed syringe pump within 1 h under strong agitation to obtain

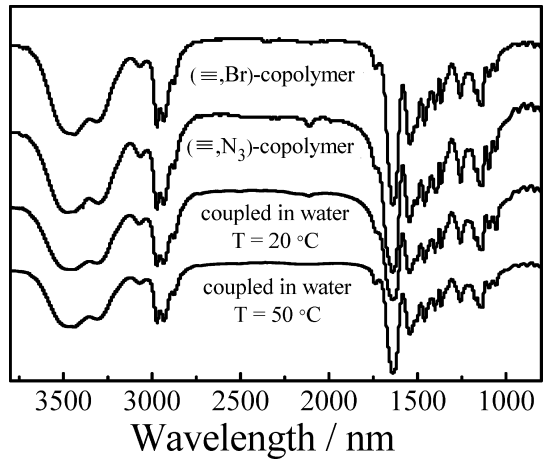

Figure 6. IR spectra of (≡,Br)-PNIPAM-*b*-PDMA, (≡,N_3)-PNIPAM-*b*-PDMA, and star-like (PNIPAM-*b*-PDMA)$_n$ prepared at different temperatures.

a solution with a concentration of 0.1 g/L. Note that when the copolymer concentration is higher than 0.5 g/L, precipitation occurs. The solution was kept at ~10 °C and bubbled with nitrogen for ~30 min to remove oxygen. After the addition of sodium ascorbate (0.025 g, 0.12 mmol) and $CuSO_4$ (10 mg, 0.06 mmol), the reaction mixture was stirred for 24 h under N_2 at ~10 °C. The rest purification procedure is similar as before.

RESULTS AND DISCUSSION

Figure 1 shows that the RAFT agent (**I**) with three reactive groups (alkyne, thiocarbonylthio, and bromine) was fairly pure, where the calculated area ratio of peak *e*, peak *c*, and peak *g* is 1.00/2.95/2.98, agreeing well with its theoretical value of 1.00/3.00/3.00. The SEC results in the inset shows a narrowly distributed peak ($M_{n,app}$ = 6.00 × 10^2 g/mol and M_w/M_n = 1.02). The details of its preparation and ^{1}H NMR spectra of other intermediate compounds generated in the process can be found in the Supporting Information (Figure S1).

Figure 2 shows that using the RAFT polymerization, narrowly distributed homopolymer (≡,Br)-PNIPAM and diblock copolymer (≡,Br)-PNIPAM-*b*-PDMA were prepared in dioxane. The degrees of polymerization (*DP*) of PNIPAM and PDMA blocks were calculated from the area ratio of peak *a*, peak *b*, and peak *c*, as shown in Figure 3, i.e., $DP_{PNIPAM} = 2(A_a/A_c)$ = ~41 and $DP_{PDMA} = (A_b/A_c)/3$ = ~58. It should be stated that the weight-average molar mass of (≡,Br)-PNIPAM-*b*-PDMA from SEC ($M_{w,SEC}$ = 1.28 × 10^4 g/mol) is slightly higher than that calculated from ^{1}H NMR spectrum ($M_{w,NMR} = M_{n,NMR} \times (M_w/M_n)_{SEC}$ = 1.10 × 10^4 g/mol).

As shown in Figure 4, before treated with a mixture of AIBN and BPO, (≡,Br)-PNIPAM-*b*-PDMA chains aggregate to form a structure with an average hydrodynamic radius ($\langle R_h \rangle$) of ~54 nm at 50 °C (much higher than the lower critical solution temperature, LCST, of PNIPAM in water). Such formed aggregates are broadly distributed and much larger than its expected core−shell micelle-like structure since individual copolymer chains in THF (a good solvent) only have a size of 2−3 nm and their contour length is shorter than 30 nm, indicating that the hydrophobic end ($-C_{12}H_{25}$) unexpectedly affects the self-assembly of the copolymer chains.

Therefore, we have to remove this hydrophobic end by treating (≡,Br)-PNIPAM-*b*-PDMA with a mixture of excess of AIBN and BPO via the RAFC process.[37,38] As shown in Figure

dx.doi.org/10.1021/ma401675q | *Macromolecules* 2013, 46, 8152−8160

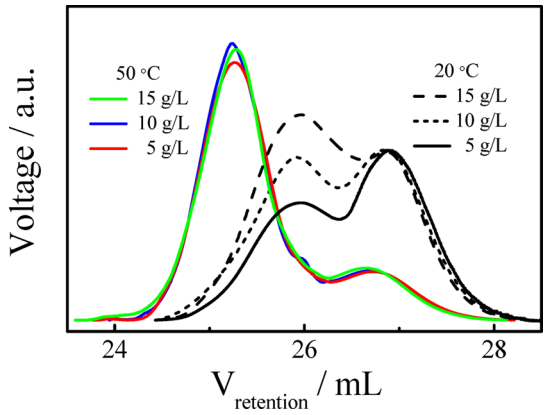

Figure 7. SEC curves of star-like (PNIPAM-*b*-PDMA)$_n$ copolymers prepared at different temperatures and initial macromonomer concentrations.

5, the peak associated with trithiocarbonate (at ∼310 nm) completely disappears for a given polymer concentration after the copolymer is treated with an optimal mixture of AIBN and BPO (50/2). Note that if AIBN is used alone, 200 mol equiv is not sufficient to displace the thiocarbonylthio group from the chain end, presumably due to the poorer leaving ability of radicals generated from AIBN. It should be noted that the bromine atoms should remain intact during the RAFT and RAFC processes in principle, which is supported by many previous studies[39−42] and the successful installation of azide groups in the next step. As expected, no biradical coupling termination was observed during the RAFC process (Figure 2).

Further substitution of the bromine end group with an azide group leads to a diblock copolymer (≡,N_3)-PNIPAM-*b*-PDMA. The reaction is efficient and completed within a short time. As shown in Figure 4, after the removal of large hydrophobic $-C_{12}H_{25}$ end group, individual (≡,N_3)-PNIPAM-*b*-PDMA chains can self-assemble into a much smaller and narrowly distributed core−shell micelle-like structure with $\langle R_h \rangle \sim 18$ nm in water at 50 °C which is much higher than the LCST (∼32 °C) of PNIPAM in water. Moreover, using static LLS, we estimated that such formed polymeric micelles have a weight-average molar mass of $M_w \sim 8.9 \times 10^5$ g/mol (Figure S2) and the average aggregation number (N_{agg}) is ∼80, calculated from the ratio of $M_{w,micelle}/M_{w,unimer}$, i.e., each micelle contains ∼80 PNIPAM-*b*-PDMA chains.

After solving the self-assembly problem, we were able to study the effect of self-assembly on the interchain coupling ("click") of (≡,N_3)-PNIPAM-*b*-PDMA chains in aqueous solutions by purposely choosing two reaction temperatures much higher or lower than the self-assembly temperature (∼32 °C). It is worth-noting that the copolymer concentration used was 5−15 g/L, much lower than those typically employed in previous interchain coupling experiments.[43−45] Figure 6 unexpectedly shows that the characteristic absorbance peak (2110 cm^{-1}) of azide groups becomes smaller after the coupling at 20 °C without the self-assembly. In comparison, the peak completely disappears after the coupling at 50 °C with the self-assembly. The "click" coupling reaction successfully proceeded in both conditions.

However, Figure 7 shows that the resultant star-like (PNIPAM-*b*-PDMA)$_n$ copolymers prepared at 20 and 50 °C have very different elution curves, which implies the previous observed disappearance of the characteristic absorbance peaks of azide groups at 20 °C is attributed to both the contributions of interchain reaction and intrachain cyclization. As shown in Figure 7, the coupling products formed at 20 °C have a bimodal distribution with lots of uncoupled individual copolymer chains and their weight-average molar masses gradually and typically increase with the copolymer concentration. In contrast, the resultant coupling products obtained with the self-assembly at 50 °C have a similar elution curves and their $M_{w,SEC}$ values are independent of the copolymer concentration (C), which is due to the facts that (1) the interchain coupling reaction mainly occurs inside the well-defined core (a nanoreactor, <10 nm^3) and (2) the micelle formation in dilute solutions is mainly thermodynamically governed so that the increase of C above its critical micelle concentration (CMC) mainly results in more polymeric micelles but has less effects on either their average associate number or structure. Namely, the concentration of the reactive end groups inside the core of each micelle nearly remains a constant.

Figure 7 also shows that at $C_{copolymer}$ = 10 g/L, the interchain coupling at 50 °C leads to a star-like (PNIPAM-*b*-PDMA)$_n$ copolymer with a weight-average molar mass ($M_{w,SEC} = 6.05 \times 10^4$ g/mol), three times higher than those prepared at 20 °C, which clearly indicates that the self-assembly assists the interchain coupling of individual initial diblock chains [(≡,N_3)-PNIPAM-*b*-PDMA] into a star-like copolymer [(PNIPAM-*b*-PDMA)$_n$]. Note that here individual copolymer chains are further "polymerized" together. This is why we have coined a word "polypolymerization" and the term SAAP to reflect its nature. It should be emphasized that the hydrodynamic size of a star-like chain is much smaller than its linear counterpart with an identical overall molar mass.[14] Therefore, the size-exclusion based method unavoidably underestimated its true molar mass.[14,46−49] One has no choice but using an absolute method, such as static LLS, to characterize these branched copolymers. Unfortunately, it has been ignored by most of polymer chemists in current literatures.

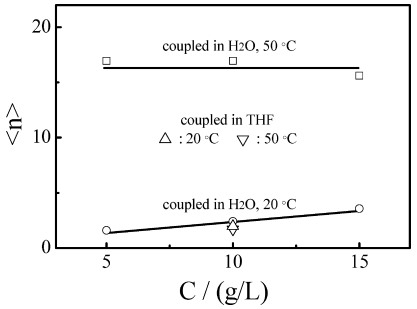

Figure 8. Initial macromonomer concentration (C) dependence of average number ($\langle n \rangle$) of macromonomer chains per star-like (PNIPAM-*b*-PDMA)$_n$ prepared at different temperatures, where $\langle n \rangle$ has a relative error of ±10%.

Figure 8 clearly shows that the star-like copolymers prepared with the self-assembly at 50 °C have a much higher average number of linear macromonomers per star-like chain ($\langle n \rangle$) than those made without the self-assembly, where $\langle n \rangle$ can be calculated as follows: $\langle n \rangle = M_{w,star}/M_{w,diblock}$. Moreover, $\langle n \rangle$ nearly remains a constant with the self-assembly but slightly increases without the self-assembly as the initial macromonomer concentration increases. Such a difference has already been explained. Quantitatively, with the assistant of self-assembly, ∼17 linear macromonomer (≡,N_3)-PNIPAM-*b*-

dx.doi.org/10.1021/ma401675q | *Macromolecules* 2013, 46, 8152−8160

PDMA chains were coupled together in the core to form a star-like (PNIPAM-*b*-PDMA)$_n$ chain, while with no self-assembly, the reaction only couples few linear (≡,N_3)-PNIPAM-*b*-PDMA chains together to form di- and trimers.

A combination of SEC and LLS results reveals that on average about one-fifth of ~80 (≡,N_3)-PNIPAM-*b*-PDMA chain ends are coupled together to form a star-like copolymer chain. In other words, initial ~80 macromonomer chains inside each micelle are coupled into 4−5 star-like copolymer chains. The failure to couple all of them into one larger star-like chain should be attributed to the low mobility of the collapsed PNIPAM blocks inside the core and fewer reactive groups (4−5) that were left inside each core after most of the chain ends are coupled together. Note that there always exists an intrachain coupling possibility, especially when the interchain "click" reaction reaches its end.

An attentive reader might ask whether the coupling reaction temperature, instead of the self-assembly, plays a dominant role here, i.e., a higher reaction temperature leads to a higher reactivity of the chain ends. To answer it, we did control experiments in a good solvent (THF) at two different temperatures (20 and 50 °C), where the reaction condition is [azide]/[CuBr]/[PMDETA] = 1/10/10. The results are also plotted in Figure 8. It is clear that the reaction temperature has no effect on the interchain coupling of linear (≡,N_3)-PNIPAM-*b*-PDMA chains without the assistant of self-assembly. Therefore, we can confidently state that it is the self-assembly that concentrates the reactive groups at the chain end into the core and assists the interchain coupling reaction.

It is also worth-noting that our previous studies of the coil-to-globule transition of individual long linear PNIPAM chains in water revealed that the inside of each collapsed chain is not as dry as we thought but contains ~70−80% of water.[50−54] In other words, the PNIPAM blocks inside the core are not as frozen as one might thought, which explains why we are still able to couple a number of macromonomer chains inside together. After separating the low molar mass fraction and those uncoupled macromonomer chains from the resultant star-like copolymer by the precipitation fractionation in a mixture of THF and hexane, we obtained a star-like copolymer with a higher molar mass, and on average, each star-like chain contains ~22 linear PNIPAM-*b*-PDMA "arms". Using this high molar mass sample, we further studied its temperature dependent intrachain folding and interchain association in water by using a combination of static and dynamic LLS.

Parts A and B of Figures 9 show that as the solution temperature increases from 25 to 55 °C, both the weight-average molar mass (M_w) and the average hydrodynamic radius ($\langle R_h \rangle$) slightly increase, indicating weak chain association. On average, each aggregate contains less than two star-like (PNIPAM-*b*-PDMA)$_{22}$ chains. In comparison, under identical experimental conditions (temperature and concentration), the association number of its linear copolymer precursors, (≡,N_3)-PNIPAM-*b*-PDMA, is ~80. Such a huge difference is understandable because further interchain aggregation of those collapsed PNIPAM blocks inside a star-like chain at higher temperatures (>32 °C) in water is likey prevented by those hydrophilic PDMA shell. A similar phenomena was also seen in previous studies of the interchain association of amphiphilic star-like copolymers in dilute solutions.[55,56] The slight decrease of the average chain density ($\langle \rho \rangle$) (Figure 9C) reveals that the association of star-like amphiphilic copolymer chains leads to lose interchain aggregates.

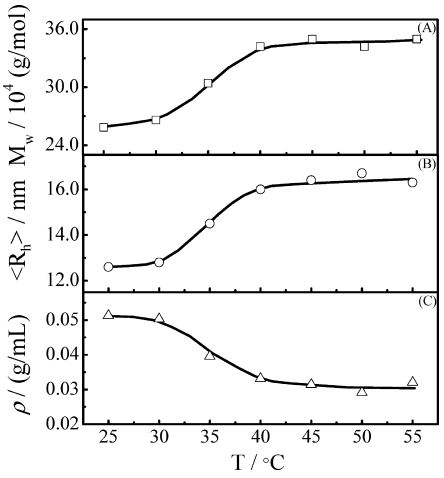

Figure 9. Temperature dependence of (A) apparent weight-average molar mass (M_w), (B) average hydrodynamic radius ($\langle R_h \rangle$), and (C) average chain density ($\langle \rho \rangle$) of star-like amphiphilic copolymer (PNIPAM-*b*-PDMA)$_{22}$ in water, where $C_{polymer}$ = 1.0 g/L and $\langle \rho \rangle$ is calculated from $3M_w/(4\pi\langle R_h \rangle^3)$.

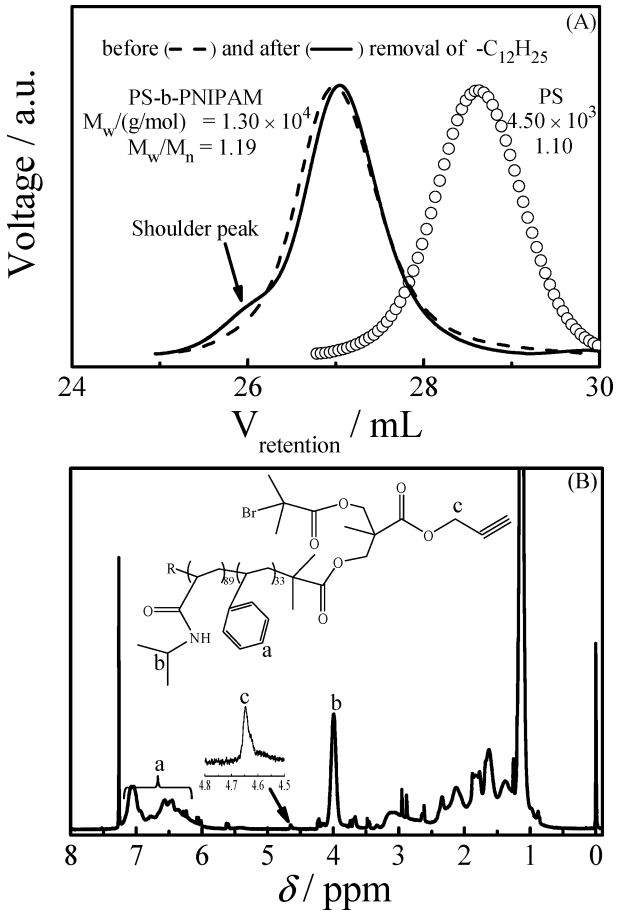

Figure 10. (A) SEC curves of PS and PS-*b*-PNIPAM-$C_{12}H_{25}$ before and after treatment with AIBN and BPO and (B) ^{1}H NMR spectrum of (≡,Br)-PS-*b*-PNIPAM in $CDCl_3$.

Up to now, we have demonstrated that the interchain coupling of linear macromonomer (≡,N_3)-PNIPAM-*b*-PDMA chains in aqueous solutions is also enhanced in the collapsed PNIPAM core in water. Further, we like to study such an enhancement in organic solvents by purposely synthesizing

dx.doi.org/10.1021/ma401675q | *Macromolecules* 2013, 46, 8152−8160

(≡,N_3)-PS-*b*-PNIPAM diblock chains. As shown in Figure 10A, linear PS_{33}-*b*-$PNIPAM_{89}$ diblock chains are narrowly distributed with an apparent M_w of 1.30×10^4 g/mol, where the absolute degrees of polymerization of PS and PNIPAM blocks were calculated from ^{1}H NMR spectrum (Figure 10B). Note that there is a small shoulder located at 2.70×10^4 g/mol (M_w) after the removal of the $-C_{12}H_{25}$ end group, presumably due to some biradical coupling induced termination.

Further, we comparatively studied the interchain association and coupling of (≡,N_3)-PS-*b*-PNIPAM chains in THF, water, methanol and 2-propanol. The latter three solvents are selectively good for PNIPAM but poor for PS at 20 °C in the order: water (poorest) < methanol (poorer) < 2-propanol (poor). Experimentally, we dissolved PS-*b*-PNIPAM in alcohols at 60 °C and then cooled the solution down to induce the self-assembly. On the other hand, we gradually added a THF solution of (≡,N_3)- PS-*b*-PNIPAM into water to induce the self-assembly. Judging from the measured $\langle R_h \rangle$ of those assembled structures in Figure 11A, we realize that a core–shell micellar structure is formed only in methanol.

The small peak located at ~3 nm in 2-propanol indicates that there exist lots of unassembled initial macromonomer chains because the peak area is weighed by the intensity of the scattered light, not the number of the chains. In water, the measured $\langle R_h \rangle$ is ~76 nm, larger than a fully stretched PS_{33}-*b*-$PNIPAM_{89}$ chain with a contour length of ~35 nm, which presumably indicates the formation of some large aggregates because the final state of such an assembled structure made of amphiphilic chains with an extremely solvophobic block is kinetically, not thermodynamically, controlled by the preparation process.[57,58] Note that the N═N═N antisymmetric stretch of star-like copolymer chains prepared in THF, methanol and 2-propanol nearly disappears after the interchain coupling (Figure S4). In contrast, the change in water is not observable, presumably because 1) the collapsed PS blocks are frozen in water in each microdomain; and 2) most of water-soluble catalyzers are not able to diffuse into the hydrophobic PS microdomains to effectively promote the azide–alkyne "click" reaction.

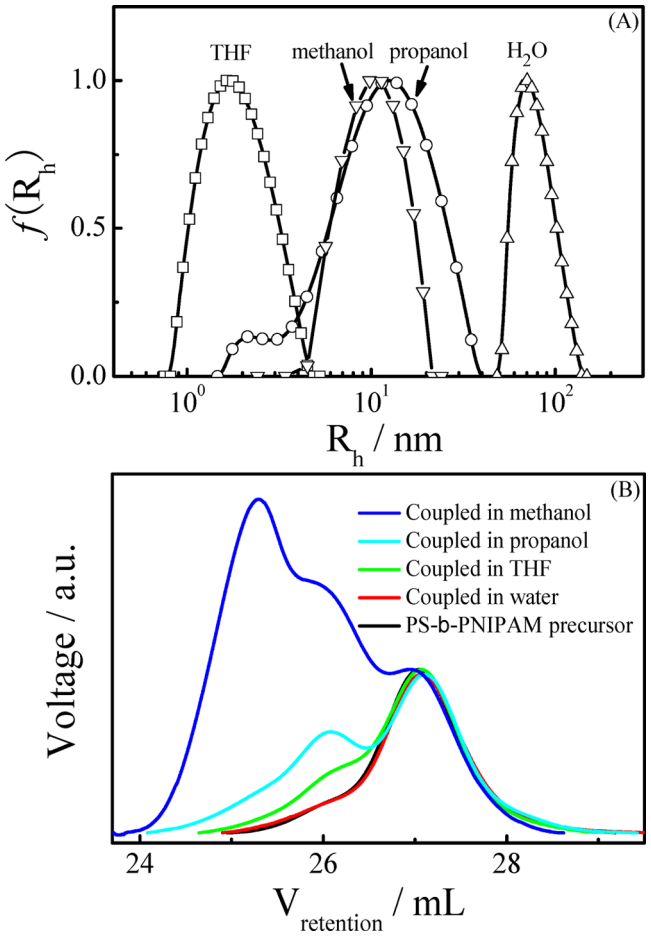

Figure 11. (A) Hydrodynamic radius distributions ($f(R_h)$) of PS-*b*-PNIPAM in various solvents; and (B) SEC curves of star-like (PS-*b*-PNIPAM)$_n$ chains prepared without self-assembly (25 °C in organic solvents) and with self-assembly (20 °C in water).

Figure 11B shows that a significant improvement of the interchain coupling efficiency only occurs in methanol, while the retention peaks of dimer and initial unimer chains still dominate in THF (no self-assembly) and 2-propanol (a mixture of unimers and micelles). The measured $\langle n \rangle$ values of star-like (PS-*b*-PNIPAM)$_n$ are 5.3 (methanol) and 1.2 (2-propanol). There is nearly no coupling in either THF or water, indicating that both the self-assembly and the chain mobility in the core are important for an effective interchain coupling. In addition, a relatively lower catalytic efficiency of the copper-based catalyst in nonaqueous solution also affects the coupling efficiency.[59] It is interesting to note that before the interchain coupling, the apparent N_{agg} in methanol is 18, much smaller than that in pure water (~1700) (Figure S2), clearly revealing that it is the well-defined self-assembled structure and the mobility of the insoluble blocks, but not the random association, that play critical and important roles in the promotion of the interchain coupling reaction.

To further investigate such an effect of the solvent quality on the interchain coupling effeciency, we studied the interchain association and interchain coupling of linear macromonomer PS-*b*-PNIPAM in different mixtures of water and 2-propanol that has a fixed amount. Figure 12 shows that the peak related

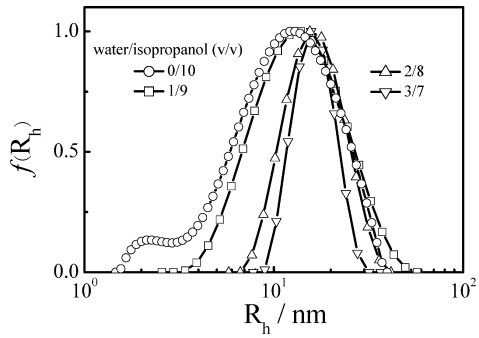

Figure 12. Hydrodynamic radius distributions ($f(R_h)$) of PS-*b*-PNIPAM chains in water/2-propanol mixtures with different water volume fractions, where $C_{copolymer}$ = 5 g/L.

to the macromonomer (~3.0 nm) gradually dissapears as more water is added and a narrow peak located at ~15 nm appears when the water content is higher than 20 v/v%, reflecting the formation of the well-defined core–shell micelles. Further increase of the water content (>40 v/v%) resulted in the macroscopic precipitation of the macromonomer chains (Figure S5). At the same time, the apparent average aggregation number characteried by static LLS gradually increases from 4 to 33 as the water content increases from 0 to 30 v/v%.

dx.doi.org/10.1021/ma401675q | *Macromolecules* 2013, 46, 8152–8160

Figure 13 shows that the average number $\langle n \rangle$ of macromonomer PS-*b*-PNIPAM chains coupled inside each star-like

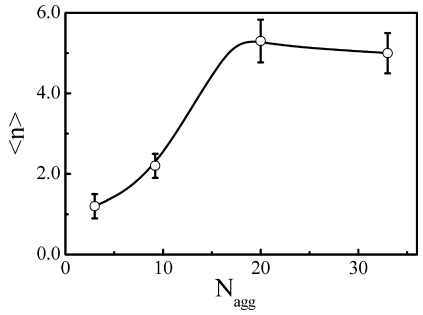

Figure 13. Average aggregation number (N_{agg}) dependence of coupling efficiency in terms of average number ($\langle n \rangle$) of macromonomer chains per star-like (PS-*b*-PNIPAM)$_n$ prepared in different water/2-propanol mixtures at 25 °C.

copolymer (PS-*b*-PNIPAM)$_n$ chain increases with N_{agg} inside each self-assembled/aggregated structure before the coupling reaction, i.e., increases with the water content and levels off at ~20 v/v%. This result reveals that the self-assembly into the core−shell micelle-like structure can indeed help the interchain coupling. It is worth-noting once more that both the self-assembly and the chain mobility inside the insoluble phase are governed by the solvent quality and they have opposite effects on the coupling effeciency inside the core or the insoluble domain.

CONCLUSION

The self-assembly of amhiphilic diblock copolymer chains in a selective solvent can lead to an effective interchain coupling (polypolymerization) of reactive groups at the insoluble block ends as long as a delicate balance between the self-assembly and the mobility of the collapsed blocks is established by properly adjusting the solvent quality. Namely, the solvent should be sufficiently selective but not too poor for the insoluble block so that its insolubility will lead to the self-assembly to form a core−shell micelle-like structure but not the frozen of the chain ends inside the core. We have demonstrated that using such the self-assembly assisted polypolymerization (SAAP) is able to couple 5−20 (≡,N_3)-poly(*N*- isopropylacrylamide)-*b*-poly(*N*,*N*-dimethylacrylamide) [(≡,N_3)-PNIPAM-*b*-PDMA] or (≡,N_3)-polystyrene-*b*-poly(*N*-iso-propylacrylamide) [(≡,N_3)-PS-*b*-PNIPAM] chains together to form a star-like multiblock (PNIPAM-*b*-PDMA)$_n$ or (PS-*b*-PNIPAM)$_n$ chain. Note that in principle the SAAP can be used to make chains with other topologies, depending on which reactive groups are used and where they are located in the initial macromonomer chains. Scheme 3 schemetically illustrats few, but not limited, possibilities.

Scheme 3. Schematic of Self-Assembly Assisted Polypolymerization (SAAP) Strategy Used to Synthesize Amphiphilic Copolymers with Different Topologies

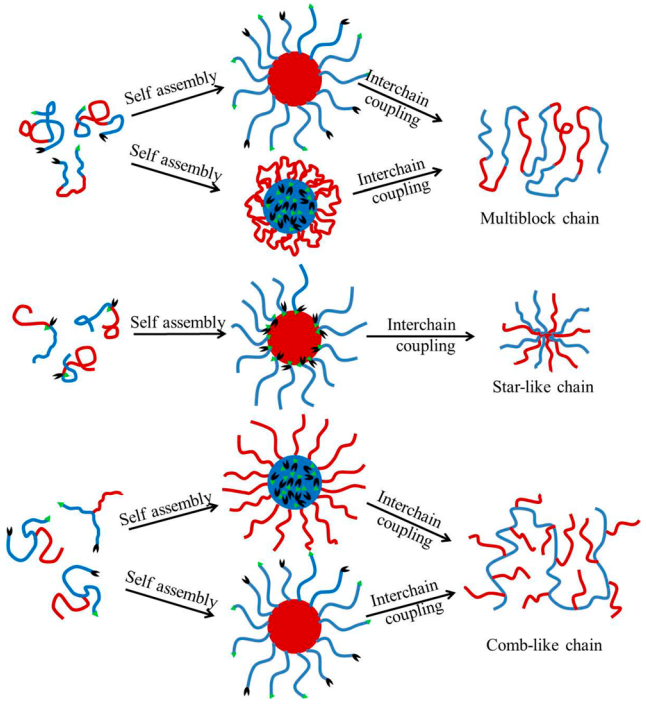

ASSOCIATED CONTENT

Supporting Information

The detailed experimental procedures of synthesis of RAFT agent and other characterization results. This material is available free of charge via the Internet at http://pubs.acs.org.

AUTHOR INFORMATION

Corresponding Authors

*E-mail: (L.L.) llw@mail.ustc.edu.cn.
*E-mail: (C.W.) chiwu@cuhk.edu.hk.

Notes

The authors declare no competing financial interest.

ACKNOWLEDGMENTS

The financial support of the National Natural Scientific Foundation of China Projects (20934005 and 51173177), the Ministry of Science and Technology of China Key Project (2012CB933802), and the Hong Kong Special Administration Region Earmarked Projects (CUHK4036/11P, 2130281/2060431; CUHK7/CRF/12G, 2390062) is gratefully acknowledged.

REFERENCES

(1) Xu, J.; Ye, J.; Liu, S. *Macromolecules* **2007**, *40*, 9103.
(2) Misaka, H.; Kakuchi, R.; Zhang, C.; Sakai, R.; Satoh, T.; Kakuchi, T. *Macromolecules* **2009**, *42*, 5091.
(3) Yamazaki, Y.; Ajioka, N.; Yokoyama, A.; Yokozawa, T. *Macromolecules* **2009**, *42*, 606.
(4) Zhao, J.; Schlaad, H. *Macromolecules* **2011**, *44*, 5861.
(5) Hu, J.; Ge, Z.; Zhou, Y.; Zhang, Y.; Liu, S. *Macromolecules* **2010**, *43*, 5184.
(6) Xia, J.; Matyjaszewski, K. *Macromolecules* **1997**, *30*, 7697.
(7) Trollsas, M.; Atthoff, B.; Claesson, H.; Hedrick, J. *Macromolecules* **1998**, *31*, 3439.
(8) Trollsås, M.; Hedrick, J. *Macromolecules* **1998**, *31*, 4390.
(9) Hutchings, L.; Dodds, J.; Roberts-Bleming, S. *Macromolecules* **2005**, *38*, 5970.
(10) Hutchings, L.; Dodds, J.; Roberts-Bleming, S. *Macromol. Symp.* **2006**, *240*, 56.
(11) Hutchings, L. *Soft Matter* **2008**, *4*, 2150.
(12) Kim, Y.; Webster, O. *J. Am. Chem. Soc.* **1990**, *112*, 4592.
(13) Kim, Y.; Webster, O. *Macromolecules* **1992**, *25*, 5561.
(14) Li, L.; He, C.; He, W.; Wu, C. *Macromolecules* **2011**, *44*, 8195.

(15) Killops, K.; Campos, L.; Hawker, C. *J. Am. Chem. Soc.* **2008**, *130*, 5062.
(16) Hanisch, A.; Schmalz, H.; Müller, A. *Macromolecules* **2012**, *45*, 8300.
(17) Gao, H.; Matyjaszewski, K. *Macromolecules* **2006**, *39*, 3154.
(18) Gao, H.; Matyjaszewski, K. *Macromolecules* **2008**, *41*, 4250.
(19) Dong, Z.; Liu, X.; Liu, H.; Li, Y. *Macromolecules* **2010**, *43*, 7985.
(20) Ferreira, J.; Syrett, J.; Whittaker, M.; Haddleton, D.; Davis, T.; Boyer, C. *Polym. Chem.* **2011**, *2*, 1671.
(21) Gao, H.; Matyjaszewski, K. *J. Am. Chem. Soc.* **2007**, *129*, 6633.
(22) Quémener, D.; Hellaye, M.; Bissett, C.; Davis, T.; Barner-Kowollik, C.; Stenzel, M. *J. Polym. Sci., Part A: Polym.Chem.* **2008**, *46*, 155.
(23) Zhang, J.; Zhou, Y.; Zhu, Z.; Ge, Z.; Liu, S. *Macromolecules* **2008**, *41*, 1444.
(24) Goldmann, A.; Walther, A.; Nebhani, L.; Joso, R.; Ernst, D.; Loos, K.; Barner-Kowollik, C.; Barner, L.; Muller, A. *Macromolecules* **2009**, *42*, 3707.
(25) Touris, A.; Hadjichristidis, N. *Macromolecules* **2011**, *44*, 1969.
(26) Wan, X.; Liu, T.; Liu, S. *Biomacromolecules* **2011**, *12*, 1146.
(27) Liu, X.; Luo, S.; Ye, J.; Wu, C. *Macromolecules* **2012**, *45*, 4830.
(28) Wu, C.; Xie, Z.; Zhang, G.; Zi, G.; Tu, Y.; Yang, Y.; Cai, P.; Nie, T. *Chem. Commun.* **2002**, *38*, 2898.
(29) Zhu, F.; Ngai, T.; Xie, Z.; Wu, C. *Macromolecules* **2003**, *36*, 7405.
(30) Wang, W.; Li, T.; Yu, T.; Zhu, F. *Macromolecules* **2008**, *41*, 9750.
(31) Hong, L.; Zhu, F.; Li, J.; Ngai, T.; Xie, Z.; Wu, C. *Macromolecules* **2008**, *41*, 2219.
(32) Guo, A.; Liu, G.; Tao, J. *Macromolecules* **1996**, *29*, 2487.
(33) Rheingans, O.; Hugenberg, N.; Harris, J. R.; Fischer, K.; Maskos, M. *Macromolecules* **2000**, *33*, 4780.
(34) Njikang, G.; Liu, G.; Hong, L. *Langmuir* **2011**, *27*, 7176.
(35) Tao, J.; Liu, G. *Macromolecules* **1997**, *30*, 2408.
(36) Hu, J.; Zheng, R.; Wang, J.; Hong, L.; Liu, G. *Macromolecules* **2009**, *42*, 4638.
(37) Chong, Y.; Moad, G.; Rizzardo, E.; Thang, S. H. *Macromolecules* **2007**, *40*, 4446.
(38) Chen, M.; Moad, G.; Rizzardo, E. *J. Polym. Sci., Part A: Polym.Chem.* **2009**, *47*, 6704.
(39) Bolton, J.; Rzayev, J. *ACS Macro Letters* **2011**, *1*, 15.
(40) Nese, A.; Li, Y.; Sheiko, S. S.; Matyjaszewski, K. *ACS Macro Lett.* **2012**, *1*, 991.
(41) Stals, P. J. M.; Li, Y.; Burdyńska, J.; Nicolaÿ, R.; Nese, A.; Palmans, A. R. A.; Meijer, E. W.; Matyjaszewski, K.; Sheiko, S. S. *J. Am. Chem. Soc.* **2013**, *135*, 11421.
(42) Zhang, Y.; Shen, Z.; Yang, D.; Feng, C.; Hu, J.; Lu, G.; Huang, X. *Macromolecules* **2009**, *43*, 117.
(43) Kricheldorf, H. *Macromol. Rapid Commun.* **2008**, *29*, 1695.
(44) Konkolewicz, D. *Aust. J. Chem.* **2009**, *62*, 823.
(45) Kricheldorf, H. *Macromol. Rapid Commun.* **2009**, *30*, 1371.
(46) Teraoka, I. *Macromolecules* **2004**, *37*, 6632.
(47) Wang, Y.; Teraoka, I.; Hansen, F.; Peters, G.; Hassager, O. *Macromolecules* **2010**, *43*, 1651.
(48) Wang, Y.; Teraoka, I.; Hansen, F.; Peters, G.; Hassager, O. *Macromolecules* **2010**, *43*, 403.
(49) Pomposo, J. A.; Perez-Baena, I.; Buruaga, L.; Alegría, A.; Moreno, A. J.; Colmenero, J. *Macromolecules* **2011**, *44*, 8644.
(50) Petrov, P. D.; Drechsler, M.; Muüller, A. *J. Phys. Chem. B* **2009**, *113*, 4218.
(51) Colombani, O.; Lejeune, E.; Drechsler, M.; Jestin, J.; Müller, A.; Chassenieux, C. *Macromolecules* **2010**, *43*, 2667.
(52) Jacquin, M.; Muller, P.; Cottet, H.; Théodoly, O. *Langmuir.* **2010**, *26*, 18681.
(53) Wu, C.; Zhou, S. *Macromolecules* **1995**, *28*, 8381.
(54) Wu, C.; Zhou, S. *Macromolecules* **1995**, *28*, 5388.
(55) Chen, H.; Li, J.; Ding, Y.; Zhang, G.; Zhang, Q.; Wu, C. *Macromolecules* **2005**, *38*, 4403.
(56) Chen, H.; Zhang, Q.; Li, J.; Ding, Y.; Zhang, G.; Wu, C. *Macromolecules* **2005**, *38*, 8045.
(57) Jacquin, M.; Muller, P.; Cottet, H.; Théodoly, O. *Langmuir.* **2010**, *26*, 18681.
(58) Colombani, O.; Lejeune, E.; Drechsler, M.; Jestin, J.; Müller, A.; Chassenieux, C. *Macromolecules* **2010**, *43*, 2667.
(59) Kolb, H.; Finn, M.; Sharpless, K. *Angew. Chem., Int. Ed.* **2001**, *40*, 2004.